



1 **New Particle Formation and impact on CCN concentrations**
2 **in the boundary layer and free troposphere at the high**
3 **altitude station of Chacaltaya (5240 m a.s.l.), Bolivia**

4 C. Rose¹, K. Sellegri¹, I. Moreno², F. Velarde², M. Ramonet³, K. Weinhold⁴, R. Krejci⁵, M.
5 Andrade², A. Wiedensohler⁴, P. Ginot^{6,7} and P. Laj⁶

6 ¹ Laboratoire de Météorologie Physique CNRS UMR 6016, Observatoire de Physique du
7 Globe de Clermont-Ferrand, Université Blaise Pascal, 24 avenue des Landais, 63171 Aubière,
8 France

9 ² Universidad Mayor de San Andres, LFA-IIF-UMSA, Laboratory for Atmospheric Physics,
10 Campus Universitario Cota Cota calle 27, Edificio FCPN piso 3, Casilla 4680, La Paz,
11 Bolivia

12 ³ Laboratoire des Sciences du Climat et de l'Environnement, LSCE/IPSL, CEA-CNRS-
13 UVSQ, Université Paris-Saclay, F-91191, Gif-sur-Yvette, France

14 ⁴ Leibniz Institute for Tropospheric Research, Permoserstr. 15, 04318 Leipzig, Germany

15 ⁵ Department Environmental Science and Analytical Chemistry (ACES), Atmospheric
16 Science Unit, Stockholm University, S 10691 Stockholm, Sweden

17 ⁶ Laboratoire de Glaciologie et Géophysique de l'Environnement, UMR 5183, UGA/CNRS,
18 Grenoble, France

19 ⁷ Observatoire des sciences de l'Univers de Grenoble, UMS 222, IRD/UGA/CNRS, Grenoble,
20 France

21

22 **Abstract**

23 Global models predict that new particle formation (NPF) is, in some environments,
24 responsible for a substantial fraction of the total atmospheric particle number concentration
25 and subsequently contribute significantly to cloud condensation nuclei (CCN) concentrations.
26 NPF events were frequently observed at the highest atmospheric observatory in the world,
27 Chacaltaya (5240 m a.s.l.), Bolivia. The present study focuses on the impact of NPF on CCN
28 population. Neutral cluster and Air Ion Spectrometer and mobility particle size spectrometer
29 measurements were simultaneously used to follow the growth of particles from cluster sizes
30 down to ~2 nm up to CCN threshold sizes set to 50, 80 and 100 nm. Using measurements
31 performed between January 1 and December 31 2012, we found that 61% of the 94 analysed
32 events showed a clear particle growth and significant enhancement of the CCN-relevant
33 particle number concentration. We evaluated the contribution of NPF events relative to the
34 transport of pre-existing particles to the site. The averaged production of 50 nm particles



1 during those events was 5072 cm^{-3} , and 1481 cm^{-3} for 100 nm particles, with a larger
2 contribution of NPF compared to transport, especially during the wet season. The data set was
3 further segregated into boundary layer (BL) and free troposphere (FT) conditions at the site.
4 The NPF frequency of occurrence was higher in the BL (48%) compared to the FT (39%).
5 Particle condensational growth was more frequently observed for events initiated in the FT,
6 but on average faster for those initiated in the BL, when the amount of condensable species
7 was most probably larger. As a result, the potential to form new CCN was higher for events
8 initiated in the BL (67% against 56% in the FT). In contrast, higher CCN number
9 concentration increases were found when the NPF process initially occurred in the FT, under
10 less polluted conditions. This work highlights the competition between particle growth and
11 the removal of freshly nucleated particles by coagulation processes. The results support model
12 predictions which suggest that NPF is an effective source of CCN in some environments, and
13 thus may influence regional climate through cloud related radiative processes.

14 **1 Introduction**

15 Atmospheric aerosol particles are known to affect air quality, health (Seaton et al., 1995) and
16 climate. Beside their direct interaction with the solar and telluric radiations, aerosol particles
17 also act as condensation nuclei for cloud droplets. Cloud effects such as cloud albedo
18 (Twomey, 1977) and lifetime (Albrecht, 1989) constitute the largest uncertainty in the
19 estimation of the radiative forcing of the Earth's atmosphere (IPCC, 2013).

20 The interaction between aerosol particles and the formation of warm clouds relies on the
21 ability of the particles to serve as cloud condensation nuclei (CCN), which depends on the
22 water vapour supersaturation, particle size distribution and also the chemical composition
23 (e.g.: Roberts et al., 2010; Wex et al., 2010; Asmi et al., 2012). Besides the processing of
24 primary particles, other CCN sources were identified, such as regional new particle formation
25 (NPF) events (Kerminen et al., 2012).

26 NPF is a frequent atmospheric phenomenon including the formation of nanometer-sized
27 clusters from gaseous precursors and their subsequent growth to larger sizes (eg. Kulmala and
28 Kerminen, 2008). Typical growth rates between 1.8 and 10.7 nm h^{-1} were found for particles
29 in the range $1.5 - 20 \text{ nm}$ (Yli-Juuti et al., 2011), meaning that a few hours to a few days are
30 needed for nucleated particles to grow to CCN sizes, around $50-150 \text{ nm}$. The chance for these
31 clusters to grow to CCN sizes strongly depends on the competition between condensational
32 growth and their removal by coagulation onto pre-existing particles.



1 During the last few years, several global model investigations were dedicated to the study of
2 the CCN-size aerosol production attributed to atmospheric NPF (Makkonen et al., 2012;
3 Merikanto et al., 2009; Reddington et al., 2011; Spracklen et al., 2008). While the outcomes
4 of these different models may vary according to the way they treat NPF and aerosol particle
5 processes (Lee et al., 2013), most of them show an enhancement of the CCN number
6 concentration due to NPF, both in the boundary layer (BL) and in the free troposphere (FT).
7 Based on the study by Makkonen et al. (2012), predictions of the present day annual global
8 average CCN concentration in the BL show almost a fivefold increase when taking into
9 account NPF. According to Merikanto et al. (2009), 45% of global low-level cloud CCN at
10 0.2% supersaturation originate from nucleation, and 35% have been formed in the free and
11 upper troposphere. Slightly contrasting results are provided by Reddington et al. (2011) using
12 the global model GLOMAP against measurements conducted at 15 European ground based
13 stations in the frame of the EUCAARI project. Reddington and co-workers found that CCN-
14 sized particle concentrations in the BL were mainly driven by processes other than NPF,
15 which contributed significantly to the CCN budget at little less than a quarter of observational
16 sites included in the study.

17 However, observations to validate these predictions are scarce, especially for the FT, where
18 measurements are often technically challenging. In this context, the purpose of the present
19 study is to estimate the contribution of NPF to CCN formation at the station of Chacaltaya
20 (5240 m a.s.l., Bolivia) with a special attention in differentiating the CCN number
21 concentrations attributed to NPF occurring at the station from those attributed to particle
22 transport to the site. This analysis was performed using an indirect method based on the NPF
23 event classification previously reported by Rose et al. (2015) and particle number size
24 distribution measurements in the range 10-500 nm. In addition to global CCN number
25 concentrations, a more detailed analysis of NPF and subsequent CCN production in the BL or
26 in the FT is also reported.

27 **2 Measurements and methods**

28 **2.1 Observation site and instruments**

29 Aerosol particle number size distributions, together with routine meteorological parameters,
30 were measured at the Chacaltaya GAW station, located in a range of the Bolivian Andes at the



1 summit of Mount Chacaltaya (16°21.014' S, 68°07.886' W), 30 km North of La Paz (2
2 million inhabitants).

3 The mobility distribution of charged particles and ions ($3.2 - 0.0013 \text{ cm}^2\text{V}^{-1}\text{s}^{-1}$) and the size
4 distribution of total particles (2 – 42 nm) were measured by a Neutral cluster and Air Ion
5 Spectrometer (NAIS, Airel Ltd., Mirme and Mirme, 2013). The NAIS sampled the ambient
6 aerosol through an individual non-heated short inlet (~ 50 cm) with a 5 minute time
7 resolution. Since the NAIS was likely to overestimate particle number concentrations above
8 20 nm (Manninen et al., 2016), particles in the range from 20 nm to CCN relevant sizes were
9 preferentially measured using a mobility particle size spectrometer type TROPOS-SMPS
10 (Wiedensohler et al., 2012). The SMPS operated behind a Whole Air Inlet equipped with an
11 automatic dryer.

12 More details on the measurement site as well as the instrumental setup and the data quality
13 assurance can be found in Rose et al. (2015) and Andrade et al. (2015).

14 **2.2 Indirect method for the estimation of the NPF contribution to the CCN** 15 **production**

16 In absence of direct CCN measurements at Chacaltaya, the contribution of NPF to CCN
17 production was estimated from the continuous monitoring of the particle number size
18 distribution. This indirect method was first introduced by Lihavainen et al. (2003) and has
19 already been used in several other studies (Asmi et al., 2011; Kerminen et al., 2012; Laakso et
20 al., 2013; Laaksonen et al., 2005).

21 The basic hypothesis is that the lower cloud droplet activation diameter of aerosol particles is
22 in the range 50-150 nm for the usual supersaturations encountered in natural clouds (Asmi et
23 al., 2011, 2012; Komppula et al., 2005) including those forming at altitudes up to 3580 m
24 a.s.l., as observed at the Jungfraujoch station (Switzerland) (Hammer et al., 2014; Jurányi et
25 al., 2011). Although these conditions might be slightly different from those found in clouds
26 forming above 5000 m, we assume that on a first approach the CCN sizes previously
27 mentioned apply the same way at such altitudes. Thus, CCN number concentrations are
28 assimilated to a range of three different CN concentrations: hereafter, CCN_{high} and CCN_{low}
29 refer to the higher and lower limits of the CCN concentration estimated from the number
30 concentrations of particles larger than 50 nm and 100 nm, respectively; as additional
31 information, an intermediate CCN concentration (CCN_{med}) was deduced from the number



1 concentration of particles larger than 80 nm. The CCN production during an event was
2 obtained from the comparison of the CCN concentration N_{init} prior to and the maximum CCN
3 concentration N_{max} during the event. For each particle diameter range, N_{init} is defined as the
4 30 minute average concentration obtained at t_{init} , when nucleated particles reach the threshold
5 size, whereas N_{max} is the 30 minute average concentration calculated when the CCN
6 concentration reaches a maximum during an event, at t_{max} . The determination of N_{init} and N_{max}
7 is depicted on Fig. 1.

8 In addition to this first analysis classically used in the literature (that will be used in Section
9 3.1.1), further calculations are needed to take into consideration the geographical specificity
10 of the site. Indeed, if NPF contributes to the formation of potential new CCN, particles
11 transported to the site by diurnal forced or heat convection might also, in parallel, lead to an
12 apparent increase of the CCN number concentration. Thus, the CCN number concentrations
13 estimated using the methodology previously described, and attributed to NPF in a first
14 approach, might in fact result from both NPF and transport. The transport of particles to the
15 site is taken into account in Section 3.1.2., based on the hypothesis that similar number
16 concentrations of particles are transported to the site on event and non-event days. The
17 contribution of NPF to the production of new CCN was thus estimated from the difference
18 between the median CCN increases obtained on event (contributions from NPF and transport)
19 and non-event days (transport only). The hypothesis that the specific environmental
20 conditions on which NPF occurs are not favouring the transport from lower atmospheric
21 layers is not necessarily true, as NPF events were favoured during clear sky conditions (Rose
22 et al. 2015). Thus there is likely a bias towards an underestimation of transport from lower
23 atmospheric layers due to the fact that cloudy days are over-represented for non-event days.
24 This likely leads to an overestimation of the contribution of NPF to CCN number
25 concentrations. Nevertheless, this correction was never applied in the past, and certainly helps
26 approaching a more realistic view of the real contribution of NPF to CCN number
27 concentrations.

28 It is worth noticing that this indirect method based on particle size only provides estimations
29 of potential CCN concentrations instead of real concentrations as measured by CCN chambers
30 (Roberts and Nenes, 2005). However, for simplicity, we refer to these potential CCN as CCN
31 hereafter.



1 The selection of the NPF events to be analyzed was performed based on the following
2 criteria: only those NPF events with a clear particle growth (i.e. type I event following the
3 classification by Hirsikko et al., 2007) were considered and the days showing an eventual
4 contribution from NPF events triggered the day before were rejected. Regarding this aspect,
5 our analysis is thus a lower limit of the contribution of NPF to CCN-size relevant aerosol
6 concentrations.

7 **2.3 Method to assess the influence of the boundary layer in Chacaltaya**

8 In order to assess whether the site is under the influence of the planetary boundary layer or the
9 low free troposphere we employed the hourly-averaged value of the standard deviation of the
10 horizontal wind direction (σ_θ).

11 The value of σ_θ has been extensively used in air pollution monitoring (EPA, 2008; Mitchell,
12 1982; Mitchell and Timbre, 1979; Weber, 1997) and dispersion models as an indicator of the
13 stability of the lower atmosphere. Instable atmospheric conditions produce turbulence and
14 therefore high wind variability. Conversely, low wind variability due to stable conditions
15 produces low σ_θ values. In Chacaltaya, σ_θ was used from a mountain perspective, i.e.
16 assuming that turbulent conditions ($\sigma_\theta \geq 12.5$) reflect the influence of the BL at the observatory
17 and, contrarily, that non-turbulent (or stable) conditions are equivalent of being in the FT (σ_θ
18 < 12.5).

19 In Chacaltaya, σ_θ is obtained at the summit (5380 m a.s.l., 10 m above the surface) by means
20 of a wind vane and propeller (Young 05103) and processed directly on a CS-CR1000
21 datalogger. Sigma theta is defined as the standard deviation of the horizontal wind direction
22 itself according to Eq. (1), but its value is approximated by the Yamartino (1984) single-pass
23 method (set of Eq. (2)) directly in the datalogger.

$$24 \quad \sigma_\theta = \left[\frac{\sum_{i=1}^N (\theta_i - \theta_A)^2}{N - 1} \right]^{\frac{1}{2}} \quad (1)$$

25 where θ_i is the instantaneous wind direction and θ_A the average wind direction.



$$\begin{aligned}
 \sigma_{\theta} &= \arcsin(\varepsilon) \left[1 + \left(\frac{2}{\sqrt{3}} - 1 \right) \varepsilon^3 \right] \\
 \varepsilon &\equiv \sqrt{1 - (S^2 + C^2)} \\
 S &= \frac{1}{N} \sum_{i=1}^N \sin\theta_i \\
 C &= \frac{1}{N} \sum_{i=1}^N \cos\theta_i
 \end{aligned}
 \tag{2}$$

2 The synoptically driven change of wind direction may affect the calculation of σ_{θ} for short
 3 time periods. This low-frequency horizontal wind oscillation is called “meandering” and may
 4 produce overestimation of σ_{θ} during situations of low wind speed ($\leq 2\text{m}\cdot\text{s}^{-1}$), which usually
 5 take place during daytime in Chacaltaya. Therefore, 15-min averaged values are calculated
 6 offline according to Eq. (3) to avoid wind meandering effects.

$$\sigma_{\theta(1\text{-hr})}^2 = \frac{\sigma_{\theta(15)}^2 + \sigma_{\theta(30)}^2 + \sigma_{\theta(45)}^2 + \sigma_{\theta(60)}^2}{4}
 \tag{3}$$

8 where every $\sigma_{\theta(15x)}$ equation is a 15-minute deviation of the wind direction.

9 The threshold set for stable FT conditions is $\sigma_{\theta} \geq 12.5$, following Mitchell’s recommendations
 10 (1982). In Chacaltaya, FT conditions take place usually during night-time and before sunrise,
 11 as it would be expected for mountain sites. Nevertheless, in many cases σ_{θ} values lower than
 12 18 are observed in a persistent pattern (more than 4 hours of this condition). This may
 13 indicate the existence of a residual or interface layer (IL). This intermediate layer would not
 14 correspond neither to the FT nor the proper BL. Moreover, during the wet season, convective
 15 and unstable conditions produce more turbulence at the site, shifting the σ_{θ} towards higher
 16 values, typically below 18. Therefore other secondary site specific thresholds are applied,
 17 namely 18 and 22.5.

18 Obtained hourly dataset is then checked for consistency, in particular with black carbon
 19 measurements, and the following smoothing is applied. We establish a 4-hour window (2h
 20 before and 2h after the data point of interest) into which the following criteria are applied:

- 21 • If the σ_{θ} value is lower than 12.5 (classified as FT), but if it is the only data point in
 22 the 4-hour window, it is not considered as FT and it is reclassified as an IL point
 23 instead.
- 24 • If the σ_{θ} value is lower than 18 and 75% of the points in the 4-hour window are lower
 25 than 12.5, the point is classified as a FT point (stable).



- 1 • If the σ_0 value is lower than 22.5 and 75% of the points in the 4-hour window are
2 lower than 18, the point is classified as an IL point (this takes place mostly during the
3 wet season).

4

5 **3 Results**

6 **3.1 CCN formation from NPF**

7 3.1.1 Absolute and relative CCN production during NPF events

8 During the measurement period January 1 to December 31 2012, 147 days showing type I
9 NPF events were detected: 112 during the dry season, from May to October, and 35 during
10 the wet season, from November to April (Rose et al., 2015). Because of missing data of
11 particle number size distribution measurements, only 94 of them were further analysed (75
12 from the dry season and 19 from the wet season).

13 Over the whole year, 61% of the studied NPF events were observed to grow to CCN-relevant
14 sizes, and it is worth noticing that at Chacaltaya, when particles reached the lowest activation
15 diameter, i.e. 50 nm, they systematically grew up to at least 100 nm. During the wet season,
16 the frequency of aerosol particles originating from NPF event and reaching CCN sizes was
17 higher compared to the dry season (79 % and 56%, respectively). This last observation can be
18 ascribed to the larger growth rates which were detected during the wet season, being on
19 average enhanced by a factor 1.7 compared to the dry season (Rose et al., 2015).

20 The results reported by Asmi et al. (2011) for Pallas (560 m a.s.l., Finland) using similar
21 methodology slightly contrast with these observations. Indeed, the ability of NPF particles to
22 contribute to the CCN number concentration showed a seasonal variation but also decreased
23 with increasing activation diameter. This might be explained by a decreasing availability of
24 condensing vapours over the course of the particle growth time period. At Chacaltaya, the
25 availability of condensing gases appears to increase over a large time period, sometimes
26 reaching concentrations that trigger a second (and third) nucleation event during the same
27 day, in spite of the raising condensable sink due to the first nucleation event (Rose et al.
28 2015). Coagulation processes however lead to a decrease of CCN_{low} compared to CCN_{high} .
29 This is illustrated on Figure 2.a, which shows, for the three threshold sizes and for each
30 season, the median CCN concentration increase observed during NPF events and calculated
31 as the difference between N_{max} and N_{init} . Considering all type I event days over the whole



1 year, the median number concentration of new CCN produced by NPF during an event was
2 5072 cm^{-3} for CCN_{high} , 2254 and 1481 cm^{-3} for CCN_{med} and CCN_{low} , respectively. The
3 number concentration of new CCN was on average higher during the dry season, especially
4 for CCN_{high} .

5 Corresponding relative increases in CCN number concentration were calculated as the ratio of
6 the absolute increases previously reported over N_{init} , i.e. the 30 min average CCN number
7 concentration measured when nucleated particles initially reach the threshold sizes (Fig. 2.b).
8 NPF events were found to increase CCN concentrations by 168 to 996% at Chacaltaya, with
9 no clear differences between seasons or threshold sizes.

10 One should note that when several consecutive type I events were detected on a same day
11 (this occurred on 7 occasions), it was complex to extract the contribution of each individual
12 event, so the calculated CCN production was the result of the contribution of all events as a
13 whole. During multiple events days, the median number concentration of CCN produced was
14 on average 1.7 times higher compared to single type I event days.

15 As previously mentioned, similar methodology was used in previous studies to evaluate the
16 contribution of NPF to the CCN concentration. The average absolute CCN production from
17 NPF events at Chacaltaya is lower compared to that reported by Laaksonen et al., (2005) at
18 the station of San Pietro Capofiume located in the polluted region of the Pô valley (11 m
19 a.s.l., Italy): on the basis of 304 NPF events, the average number of new CCN produced
20 during an event are $7.3 \times 10^3 \text{ cm}^{-3}$ and $2.4 \times 10^3 \text{ cm}^{-3}$, for CCN_{high} and CCN_{low} , respectively. In
21 contrast, the values from both Chacaltaya and San Pietro Capofiume are significantly higher
22 than those reported by Kerminen et al. (2012) for the stations of Botsalano (1420 m a.s.l.,
23 South Africa), Vavihill (172 m a.s.l., Sweden), Pallas and Hyytiälä (182 m a.s.l., Finland).
24 Among these four sites, the highest CCN concentration increases are on average observed at
25 Botsalano (2500 cm^{-3} , 1400 cm^{-3} and 800 cm^{-3} for CCN_{high} , CCN_{med} and CCN_{low} ,
26 respectively), whereas Pallas displays the lowest CCN production (1000 cm^{-3} , 250 cm^{-3} and
27 150 cm^{-3} for CCN_{high} , CCN_{med} and CCN_{low} , respectively). Corresponding relative increases in
28 CCN concentrations found in the literature are always larger than 100% but never exceed
29 400%, being thus on average significantly lower than those observed at Chacaltaya. However,
30 it is worth noticing that these contrasting results may arise from the various conditions that
31 are found at the different stations, especially regarding altitude and pollution levels, thus
32 influencing NPF both in terms of strength, spatial extend and temporal evolution.



1 The potential of NPF to contribute to CCN production at high altitude was more particularly
2 investigated by Pierce et al. (2012) at Mount Whistler (2182 m a.s.l., Canada), following a
3 different approach including calculations of the probability for freshly nucleated particles to
4 reach CCN relevant sizes. Based on a five event day period, they found that in absence of
5 high coagulation/condensation sinks, up to 24% of the newly formed clusters could grow to at
6 least 100 nm, thus forming potential CCN.

7 However, as previously mentioned, the vertical transport of aerosol particles from lower
8 atmospheric levels that takes place after the onset of sunrise concurrently to NPF may
9 represent a significant contribution to the increase of CCN-relevant size particle number
10 concentrations at these mountain sites. This aspect will be addressed in the next section, in
11 which the contribution of NPF is further compared with the CCN number concentration
12 increase resulting from the transport of particles to the site.

13 The seasonal and annual CCN productions due to NPF events were estimated from 1) the
14 average fraction of type I NPF events contributing to the formation of new CCN reported
15 above, 2) the frequency of occurrence of type I NPF events at the site and 3) the average CCN
16 number concentration increase measured for those type I events during which newly formed
17 particles reached the potential CCN activation diameter. As an example, the CCN_{high}
18 production during the wet season was calculated as follows:

$$19 \quad CCN_{high-wet} = frac_{wet} \times tot_nb_{wet} \times avg_conc_{wet} = 79\% \times 35 \times 3070 = 8.48 \times 10^4 \text{ cm}^{-3} \quad (4)$$

20 where, for each season, *frac* is the fraction of NPF events producing CCN, *tot_nb* is the
21 total number of days showing type I events and *avg_conc* is the median number of new CCN
22 formed during an event. Similar calculations were done for each season and CCN class,
23 leading to the values reported in Table 1. The annual CCN production was calculated as the
24 sum of the seasonal productions.

25 Based on Table 1, the CCN production at Chacaltaya was higher during the dry season
26 compared to the wet season for all CCN classes, but especially for CCN_{high} , which was more
27 than 4 times higher compared to the wet season. The annual CCN production calculated at
28 San Pietro Capofiume is $3.4 \times 10^5 \text{ cm}^{-3}$ and $1.1 \times 10^5 \text{ cm}^{-3}$, for CCN_{high} and CCN_{low} , respectively
29 (Laaksonen et al., 2005). These values are slightly lower than those obtained at Chacaltaya,
30 despite the fact that the median number of potential new CCN formed during an event is on
31 average higher in San Pietro Capofiume. This last observation can be ascribed to the high



1 NPF frequency at Chacaltaya, together with the significant fraction of type I events and high
2 growth rates (Rose et al., 2015).

3 3.1.2 Correction for the contribution of particles transported to the site

4 The aim of this section is to evaluate the contribution of particles transported to the site to the
5 total CCN concentration and give a revised estimation of the CCN production from NPF.

6 The number concentration of CCN transported to the site was calculated using the particle
7 number size distributions recorded on non-event days. These conditions were fulfilled on 108
8 days (23 and 85 during the dry and wet season respectively) but only 78 of them (22 from the
9 dry season and 56 from the wet season) were further analysed because of instrumental
10 failures. The median diurnal variation of CCN_{high} obtained on non-event days and attributed to
11 transport is shown on Fig. 3, together with the median number concentrations obtained on
12 event days and ascribed to both NPF and transport (upper panel). Similar figures are reported
13 in the supplementary material for CCN_{med} and CCN_{low} (Figures S1 and S2). As previously
14 mentioned, the contribution of NPF to the production of new CCN was estimated from the
15 difference between the median CCN_{high} increases obtained on event and non-event days and is
16 shown on Fig. 3 (lower panel).

17 Outside of the NPF hours, the CCN number concentrations are on average similar on event
18 and non-event days for all sizes and seasons. During the dry season, transport contributes to
19 CCN_{med} and CCN_{low} to the median level of 1139 and 863 cm^{-3} , which is similar to the
20 contribution of NPF (between 1229 and 784 cm^{-3} depending on the season). In contrast,
21 CCN_{high} attributed to NPF (3197 cm^{-3}) significantly exceeds the median number of particles
22 transported to the site (1610 cm^{-3}). During the wet season, NPF is likely to be the dominant
23 CCN source, with productions of 1950, 771 and 535 cm^{-3} for CCN_{high} , CCN_{med} and CCN_{low} ,
24 respectively, compared to median concentrations attributed to transport which do not exceed
25 690, 404 and 321 cm^{-3} .

26 As expected, these revised NPF contributions are decreased compared to the values reported
27 on Fig. 2.a. As a consequence, the corrected seasonal and annual CCN productions ascribed to
28 NPF and reported in Table 2 are also decreased compared to the values shown in Table 1.
29 However, the revised NPF contributions still remain comparable or even higher than those
30 previously mentioned for other stations, and which probably also include CCN sources other
31 than NPF.



1 **3.2 How layering influences growth to CCN-sizes**

2 **3.2.1 Occurrence of NPF in the different tropospheric layers**

3 The purpose of this section is to further investigate NPF in terms of occurrence, event type
4 and characteristics (particle formation and growth rate) regarding the location of the station in
5 the tropospheric layers (i.e. BL, FT or IL) at the onset of the NPF process. The classification
6 of air mass types into BL, IL and FT was obtained using the Pasquill-Gifford method, which
7 uses the turbulence from the standard deviation of wind direction (Section 2.2).

8 389 NPF events previously discussed by Rose et al. (2015) were included in this analysis. For
9 each event, the air mass type (BL, IL or FT) prevailing at the station was investigated on an
10 hourly basis during the first steps of the NPF process, i.e. from the appearance of the newly
11 formed clusters (< 3nm) to the time at which the concentration of 3-7 nm particles was
12 maximum. Various scenarios were observed during this part of the NPF process, which on
13 average lasted for 2.7 ± 1.3 hours. These scenarios are listed, together with their frequency of
14 occurrence, in Table 3. Scenarios S1- S3 refer to those days when the initial steps of the NPF
15 process were observed to occur in the same atmospheric layer (respectively in the BL, in the
16 IL and in the FT). In contrast, scenarios S4 – S9 depict the situations when BL dynamics lead
17 to changing conditions in the course of the event, with a gradual evolution from BL to FT (S7
18 – S9) or vice versa (S4 - S6). S10 refers to events occurring in conditions changing randomly.
19 Since multiple events were frequently detected at Chacaltaya, additional information
20 regarding the occurrence of the scenarios as a function of the event position (first event,
21 second event, third and following events) is also provided. For that purpose, single events and
22 events occurring first on multiple event days were considered all together, while second and
23 following events were considered in a second category. There was no information available
24 regarding the classification into BL, IL and FT for 15 events.

25 Based on Table 3, constant conditions, i.e. scenarios S1 (BL conditions only), S2 (IL
26 conditions only) and S3 (FT conditions only), were found in 57% of the observed single and
27 first position events and 93% of the second and following events. In each case, scenario S1,
28 corresponding to BL conditions, was the most frequent, representing 89% and 94% of the
29 events initiated in constant conditions, respectively for single and first position events and for
30 second and following ones. The fact that scenarios related to changing conditions were more
31 frequently observed for single and first position events (41% compared to 7% for following



1 events), i.e. occurring earlier in the morning compared to following events, is mainly
2 explained by the development of the BL during the first part of the day, as shown on Fig. 4.
3 This figure also supports the fact that when changing conditions are observed, scenarios
4 starting in the FT, i.e. scenarios S4, S5, and S6, are the most probable for both seasons.
5 Among the multiple events days, 48 displayed consecutive events associated to scenarios
6 evolving in agreement with the BL dynamics shown on Fig. 4. The sequence S6-S1 was the
7 most frequent, observed on 23 days, following by the sequences S7-S1 (10 days) and S5-S1
8 (5 days). A unique sequence including three events was detected (S3-S6-S1).

9 NPF frequencies in the FT and in the BL were also deduced from the previous classification.
10 For that purpose, the analysis was focused on the time period 08:00 - 12:00 (Local), which
11 includes the most probable nucleation hours (Rose et al., 2015). 72 days (including both
12 event, non-event and undefined days) were rejected from the analysis because of missing
13 information regarding the location of the station in the tropospheric layers. Free tropospheric
14 conditions were detected during at least one hour on 122 days, and among these days, 48
15 showed NPF events initiated in the FT, leading to a NPF frequency of 39%. In contrast, the
16 station laid in the BL during at least one hour on 248 days, and among these days, 119
17 showed events starting in the BL, leading to a NPF frequency of 48%.

18 3.2.2 Event type and characteristics

19 An additional analysis concerning the event type (i.e. I, II or bump, Hirsikko et al., 2007) as a
20 function of the scenario was performed using the event classification from Rose et al. (2015).
21 The results of this analysis are shown on Fig. 5. More than half of the 77 events triggered in
22 the FT (scenarios S3, S4, S5 and S6, Table 3) were identified as type I events (39 events),
23 while types II and bump events were observed on 17 and 21 occasions, respectively, which
24 represent 22 and 27% of these scenarios. When considering the scenarios S3, S4, S5 and S6
25 independently from one another, we found that type I events were predominant when
26 changing conditions were detected (S4, S5 and S6), whereas they displayed similar
27 probabilities of occurrence as other event types in constant free tropospheric conditions (S3).
28 This observation suggests that the probability for type I events to occur is increased when
29 initial free tropospheric conditions are changing in the course of the events. This could be
30 explained by favorable conditions for the onset of nucleation events, followed by increased
31 input of condensable species from the BL promoting particle growth. However, this
32 hypothesis must be considered with caution regarding the limited number of events occurring



1 under scenario S3. Events starting at the interface between the BL and the FT are not
2 frequently observed (S2 and S7, 29 events), however, almost 50% of them (14 events) belong
3 to class I. Most of the remaining events occur under scenario S1, in the BL, with comparable
4 number of events belonging to class I and II (87 and 91 events, thus representing 40 and 42%
5 of scenario S1, respectively).

6 In order to further characterize the NPF events in the different atmospheric layers, statistics
7 regarding the formation rate of 2 nm particle and the growth rate (GR) in the size range 1-3
8 nm as a function of the scenarios were performed for type I events. As reported on Fig. 6,
9 NPF events initiated in the FT or at the interface between the BL and the FT show similar
10 particle formation and growth rates. Increased values are on average reported in the BL, with
11 higher variability, especially for the GR. Additional analysis was performed to investigate the
12 correlation between the GR in the size range 3-7 nm and the location of the station at the end
13 of the scenarios. However, because of an insufficient number of values for events occurring
14 under scenarios ending in the FT (scenarios S3 and S9, 4 values), these results will not be
15 further discussed.

16 We have shown so far that while higher NPF frequencies were found in the BL compared to
17 the FT, higher probabilities for type I events to occur were associated to scenarios starting in
18 the FT and ending in the BL or IL. However, when events belonging to class I are initiated in
19 the BL, they show on average higher particle formation and growth rates compared to those
20 started in the FT. Thus it is likely that on the one hand, higher amounts of gaseous precursors
21 usually associated with the BL could favor nucleation events of higher intensity and explain
22 both higher NPF frequencies and enhanced particle formation and growth rates. On the other
23 hand, cleaner conditions found in the FT at the very beginning of the NPF process may reduce
24 the sink for the newly formed clusters and favor their growth to larger sizes. This observation
25 suggests that the amount of condensable species could directly influence the occurrence of the
26 NPF process and determine the particle growth rate while the occurrence of the growth
27 process itself could rather depend on the strength of the particle sink. Overall, the difference
28 of occurrence frequency, nucleation rates and GR between FT and BL are not very large, and
29 we show that nucleation is initiated in the FT with a rather high frequency.

30 The purpose of the next section is now to investigate the impact of these NPF events on the
31 CCN number concentration in each of the atmospheric layers.



1 3.2.3 CCN production during NPF events in the different tropospheric layers

2 Based on the results discussed in section 3.1.1, 57 NPF event days showing particle growth up
3 to CCN activation diameter were detected at Chacaltaya. 13 of them were not further analyzed
4 due to missing information regarding the location of the station in the tropospheric layers. The
5 remaining 44 days were all single type I event days, among which 31 were initiated in the BL,
6 10 in the FT, 2 at the interface between the BL and the FT and 1 in random conditions. The
7 frequency of NPF contribution to the production of new CCN in the BL and in the FT was
8 calculated as the ratio of NPF events growing to the CCN sizes to the total number of type I
9 events occurring in each atmospheric layer, i.e. 46 in the BL and 18 in the FT. The resulting
10 frequency of CCN production from NPF was 67% in the BL, being slightly higher compared
11 to the FT (56%).

12 The number concentration of CCN formed during an event was also analyzed as a function of
13 the air mass type (BL, IL, or FT) prevailing at the station (Table 4). Using the three threshold
14 sizes, median CCN productions were comparable for events initiated in the BL and in the FT.
15 In contrast, the third quartiles of CCN_{med} and CCN_{low} were higher for the events initiated in
16 the FT.

17 The fact that the contribution of NPF to the formation of new CCN was more frequently
18 observed for events initiated in the BL might be explained by faster particle growths sustained
19 by higher amounts of condensable material, thus increasing the chances for particles to reach
20 CCN sizes. The tendency for CCN_{med} and CCN_{low} to reach higher values when the NPF
21 process was started in the FT can be due to smaller initial concentrations prior to the NPF
22 event, and thus weaker coagulation associated to less polluted conditions in the FT.

23 4 Conclusion

24 In this paper, the contribution of NPF to the production of potential new CCN was
25 investigated at the highest station in the world, Chacaltaya (5240 m a.s.l., Bolivia), between
26 January 1 and December 31 2012.

27 Using potential CCN activation diameters 50, 80 and 100 nm, we found that 61% of the type I
28 NPF events included in the analysis produced new CCN, with higher probabilities during the
29 wet season (79%) explained by faster particle growth. Because of coagulation on pre-existing
30 particles, the number concentration of CCN formed was observed to decrease with increasing
31 activation diameter, but the frequency of particles reaching the highest potential CCN



1 activation diameter (100nm) was not reduced compared to the lowest CCN size (50 nm).
2 When comparing the CCN production from NPF with the number concentration of CCN
3 transported to the site, we found that NPF was on average responsible for the largest
4 contribution to the CCN concentration, especially during the wet season.

5 When segregating into BL and FT air masses sampled at the site, we found slightly higher
6 NPF frequency in the BL (48%) but still an important frequency of occurrence in the FT
7 (nucleation frequency of 39%). This observation is, to our knowledge, the first of its kind.
8 Particle growth was more frequently observed for events initiated in the FT but was on
9 average faster for events started in the BL, most probably because of increased amounts of
10 condensable vapours. As a result, the chance for particles to grow up to potential CCN
11 activation diameters was higher when the NPF process occurred in the BL. In contrast, the
12 impact of NPF initiated in the FT on CCN number concentrations was higher than for NPF
13 initiated in the BL, most likely because of the decreased pollution levels and weaker
14 coagulation sink. The previous observations clearly highlight the competition that exists
15 between particle growth and their removal by coagulation processes on pre-existing particles,
16 and thus the complex balance between sources and sinks that is required to observe the
17 formation of new particles and their subsequent growth to climate relevant sizes. Such
18 conditions are often fulfilled at Chacaltaya, where NPF seems to often play a dominant role in
19 the formation of new CCN.

20

21 *Acknowledgments*

22 *This work was performed within the framework of ACTRIS2 (Aerosols, Clouds and Trace*
23 *gases Research Infra Structure Network) and was also supported by SNO CLAP, IRD, LEFE-*
24 *CHAT, OSUG@2020 as well as STINT and FORMAS funding agencies.*

25

26 **References**

- 27 Albrecht, B. A.: Aerosols, cloud microphysics, and fractional cloudiness, *Science*, 245(4923),
28 1227–1230, 1989.
- 29 Andrade, M., Zaratti, F., Forno, R., Gutiérrez, R., Moreno, I., Velarde, F., Ávila, F., Roca, M.,
30 Sánchez, M. F., Laj, P., Jaffrezo, J. L., Ginot, P., Sellegri, K., Ramonet, M., Laurent, O.,
31 Weinhold, K., Wiedensohler, A., Krejci, R., Bonasoni, P., Cristofanelli, P., Whiteman, D.,



- 1 Vimeux, F., Dommergue, A. and Magand, O.: Puesta en marcha de una nueva estación de
2 monitoreo climático en los andes centrales de Bolivia: la estación Gaw/Chacaltaya, Revista
3 Boliviana de Física, 26(26), 06–15, 2015.
- 4 Asmi, E., Kivekäs, N., Kerminen, V.-M., Komppula, M., Hyvärinen, A.-P., Hatakka, J.,
5 Viisanen, Y. and Lihavainen, H.: Secondary new particle formation in Northern Finland
6 Pallas site between the years 2000 and 2010, Atmos. Chem. Phys., 11(24), 12959–12972,
7 doi:10.5194/acp-11-12959-2011, 2011.
- 8 Asmi, E., Freney, E., Hervo, M., Picard, D., Rose, C., Colomb, A. and Sellegri, K.: Aerosol
9 cloud activation in summer and winter at puy-de-Dôme high altitude site in France, Atmos.
10 Chem. Phys., 12(23), 11589–11607, doi:10.5194/acp-12-11589-2012, 2012.
- 11 EPA: Quality Assurance Handbook for Air Pollution Measurement Systems, Volume IV:
12 Meteorological measurements, 2008.
- 13 Hammer, E., Bukowiecki, N., Gysel, M., Jurányi, Z., Hoyle, C. R., Vogt, R., Baltensperger,
14 U. and Weingartner, E.: Investigation of the effective peak supersaturation for liquid-phase
15 clouds at the high-alpine site Jungfraujoch, Switzerland (3580 m a.s.l.), Atmos. Chem. Phys.,
16 14(2), 1123–1139, doi:10.5194/acp-14-1123-2014, 2014.
- 17 Hirsikko, A., Bergman, T., Laakso, L., Dal Maso, M., Riipinen, I., Hörrak, U. and Kulmala,
18 M.: Identification and classification of the formation of intermediate ions measured in boreal
19 forest, Atmos. Chem. Phys., 7(1), 201–210, doi:10.5194/acp-7-201-2007, 2007.
- 20 IPCC: IPCC (AR5):Climate change 2013: The Physical Science Basis, Summary for
21 policymakers. Contribution of Working Group I to the Fifth Assessment report, 2013.
- 22 Jurányi, Z., Gysel, M., Weingartner, E., Bukowiecki, N., Kammermann, L. and Baltensperger,
23 U.: A 17 month climatology of the cloud condensation nuclei number concentration at the
24 high alpine site Jungfraujoch, J. Geophys. Res., 116(D10), D10204,
25 doi:10.1029/2010JD015199, 2011.
- 26 Kerminen, V.-M., Paramonov, M., Anttila, T., Riipinen, I., Fountoukis, C., Korhonen, H.,
27 Asmi, E., Laakso, L., Lihavainen, H., Swietlicki, E., Svenningsson, B., Asmi, A., Pandis, S.
28 N., Kulmala, M. and Petäjä, T.: Cloud condensation nuclei production associated with
29 atmospheric nucleation: a synthesis based on existing literature and new results, Atmos.
30 Chem. Phys., 12(24), 12037–12059, doi:10.5194/acp-12-12037-2012, 2012.
- 31 Komppula, M., Lihavainen, H., Kerminen, V.-M., Kulmala, M. and Viisanen, Y.:
32 Measurements of cloud droplet activation of aerosol particles at a clean subarctic background
33 site, Journal of Geophysical Research: Atmospheres (1984–2012), 110(D6) [online] Available
34 from: <http://www.agu.org/journals/jd/jd0506/2004JD005200/2004jd005200-t03.txt> (Accessed
35 21 February 2014), 2005.
- 36 Kulmala, M. and Kerminen, V.-M.: On the formation and growth of atmospheric
37 nanoparticles, Atmospheric Research, 90(2–4), 132–150, doi:10.1016/j.atmosres.2008.01.005,
38 2008.
- 39 Laakso, L., Merikanto, J., Vakkari, V., Laakso, H., Kulmala, M., Molefe, M., Kgabi, N.,
40 Mabaso, D., Carslaw, K. S., Spracklen, D. V., Lee, L. A., Reddington, C. L. and Kerminen,



- 1 V.-M.: Boundary layer nucleation as a source of new CCN in savannah environment, Atmos.
2 Chem. Phys., 13(4), 1957–1972, doi:10.5194/acp-13-1957-2013, 2013.
- 3 Laaksonen, A., Hamed, A., Joutsensaari, J., Hiltunen, L., Cavalli, F., Junkermann, W., Asmi,
4 A., Fuzzi, S. and Facchini, M. C.: Cloud condensation nucleus production from nucleation
5 events at a highly polluted region, Geophysical research letters, 32(6) [online] Available
6 from: <http://onlinelibrary.wiley.com/doi/10.1029/2004GL022092/full> (Accessed 21 February
7 2014), 2005.
- 8 Lee, L. A., Pringle, K. J., Reddington, C. L., Mann, G. W., Stier, P., Spracklen, D. V., Pierce,
9 J. R. and Carslaw, K. S.: The magnitude and causes of uncertainty in global model
10 simulations of cloud condensation nuclei, Atmos. Chem. Phys., 13(17), 8879–8914,
11 doi:10.5194/acp-13-8879-2013, 2013.
- 12 Lihavainen, H., Kerminen, V.-M., Komppula, M., Hatakka, J., Aaltonen, V., Kulmala, M. and
13 Viisanen, Y.: Production of “potential” cloud condensation nuclei associated with
14 atmospheric new-particle formation in northern Finland, Journal of Geophysical Research:
15 Atmospheres (1984–2012), 108(D24) [online] Available from:
16 <http://onlinelibrary.wiley.com/doi/10.1029/2003JD003887/full> (Accessed 21 February 2014),
17 2003.
- 18 Makkonen, R., Asmi, A., Kerminen, V.-M., Boy, M., Arneth, A., Hari, P. and Kulmala, M.:
19 Air pollution control and decreasing new particle formation lead to strong climate warming,
20 Atmos. Chem. Phys., 12(3), 1515–1524, doi:10.5194/acp-12-1515-2012, 2012.
- 21 Manninen, H. E., Mirme, S., Mirme, A., Petäjä, T. and Kulmala, M.: How to reliably detect
22 molecular clusters and nucleation mode particles with Neutral cluster and Air Ion
23 Spectrometer (NAIS), Atmospheric Measurement Techniques Discussions, 1–57,
24 doi:10.5194/amt-2016-25, 2016.
- 25 Merikanto, J., Spracklen, D. V., Mann, G. W., Pickering, S. J. and Carslaw, K. S.: Impact of
26 nucleation on global CCN, Atmos. Chem. Phys., 9(21), 8601–8616, doi:10.5194/acp-9-8601-
27 2009, 2009.
- 28 Mirme, S. and Mirme, A.: The mathematical principles and design of the NAIS – a
29 spectrometer for the measurement of cluster ion and nanometer aerosol size distributions,
30 Atmospheric Measurement Techniques, 6(4), 1061–1071, doi:10.5194/amt-6-1061-2013,
31 2013.
- 32 Mitchell, A. E.: A comparison of short-term dispersion estimates resulting from various
33 atmospheric stability classification methods, Atmospheric Environment (1967), 16(4), 765–
34 773, doi:10.1016/0004-6981(82)90394-8, 1982.
- 35 Mitchell, A. E. and Timbre, K. O.: Atmospheric stability class from horizontal wind
36 fluctuation, Proceedings of the LXXII Annual Meeting of the Air Pollution Control
37 Association, 79–29.2, 1979.
- 38 Pierce, J. R., Leaitch, W. R., Liggio, J., Westervelt, D. M., Wainwright, C. D., Abbatt, J. P.
39 D., Ahlm, L., Al-Basheer, W., Cziczo, D. J., Hayden, K. L. and others: Nucleation and
40 condensational growth to CCN sizes during a sustained pristine biogenic SOA event in a
41 forested mountain valley, Atmospheric Chemistry and Physics, 12(7), 3147–3163, 2012.



- 1 Reddington, C. L., Carslaw, K. S., Spracklen, D. V., Frontoso, M. G., Collins, L., Merikanto,
2 J., Minikin, A., Hamburger, T., Coe, H., Kulmala, M., Aalto, P., Flentje, H., Plass-Dülmer,
3 C., Birmili, W., Wiedensohler, A., Wehner, B., Tuch, T., Sonntag, A., O'Dowd, C. D.,
4 Jennings, S. G., Dupuy, R., Baltensperger, U., Weingartner, E., Hansson, H.-C., Tunved, P.,
5 Laj, P., Sellegri, K., Boulon, J., Putaud, J.-P., Gruening, C., Swietlicki, E., Roldin, P.,
6 Henzing, J. S., Moerman, M., Mihalopoulos, N., Kouvarakis, G., Ždímal, V., Zíková, N.,
7 Marinoni, A., Bonasoni, P. and Duchi, R.: Primary versus secondary contributions to particle
8 number concentrations in the European boundary layer, *Atmos. Chem. Phys.*, 11(23), 12007–
9 12036, doi:10.5194/acp-11-12007-2011, 2011.
- 10 Roberts, G. C. and Nenes, A.: A continuous-flow streamwise thermal-gradient CCN chamber
11 for atmospheric measurements, *Aerosol Science and Technology*, 39(3), 206–221, 2005.
- 12 Roberts, G. C., Day, D. A., Russell, L. M., Dunlea, E. J., Jimenez, J. L., Tomlinson, J. M.,
13 Collins, D. R., Shinzuka, Y. and Clarke, A. D.: Characterization of particle cloud droplet
14 activity and composition in the free troposphere and the boundary layer during INTEX-B,
15 *Atmos. Chem. Phys.*, 10(14), 6627–6644, doi:10.5194/acp-10-6627-2010, 2010.
- 16 Rose, C., Sellegri, K., Velarde, F., Moreno, I., Ramonet, M., Weinhold, K., Krejci, R.,
17 Andrade, M., Wiedensohler, A. and Laj, P.: Frequent nucleation events at the high altitude
18 station of Chacaltaya (5240 m a.s.l.), Bolivia, *Atmospheric Environment*, 102, 18–29,
19 doi:10.1016/j.atmosenv.2014.11.015, 2015.
- 20 Seaton, A., Godden, D., MacNee, W. and Donaldson, K.: Particulate air pollution and acute
21 health effects, *The Lancet*, 345(8943), 176–178, doi:10.1016/S0140-6736(95)90173-6, 1995.
- 22 Spracklen, D. V., Carslaw, K. S., Kulmala, M., Kerminen, V.-M., Sihto, S.-L., Riipinen, I.,
23 Merikanto, J., Mann, G. W., Chipperfield, M. P. and Wiedensohler, A.: Contribution of
24 particle formation to global cloud condensation nuclei concentrations, *Geophysical Research*
25 *Letters*, 35(6) [online] Available from:
26 <http://onlinelibrary.wiley.com/doi/10.1029/2007GL033038/full> (Accessed 17 October 2013),
27 2008.
- 28 Twomey, S.: The influence of pollution on the shortwave albedo of clouds, *Journal of the*
29 *atmospheric sciences*, 34(7), 1149–1152, 1977.
- 30 Weber, R. O.: Estimators for the Standard Deviation of Horizontal Wind Direction, *J. Appl.*
31 *Meteor.*, 36(10), 1403–1415, doi:10.1175/1520-0450(1997)036<1403:EFTSDO>2.0.CO;2,
32 1997.
- 33 Wex, H., McFiggans, G., Henning, S. and Stratmann, F.: Influence of the external mixing
34 state of atmospheric aerosol on derived CCN number concentrations, *Geophysical Research*
35 *Letters*, 37(10) [online] Available from:
36 <http://onlinelibrary.wiley.com/doi/10.1029/2010GL043337/full> (Accessed 21 February 2014),
37 2010.
- 38 Wiedensohler, A., Birmili, W., Nowak, A., Sonntag, A., Weinhold, K., Merkel, M., Wehner,
39 B., Tuch, T., Pfeifer, S., Fiebig, M., Fjåraa, A. M., Asmi, E., Sellegri, K., Depuy, R., Venzac,
40 H., Villani, P., Laj, P., Aalto, P., Ogren, J. A., Swietlicki, E., Williams, P., Roldin, P.,
41 Quincey, P., Hüglin, C., Fierz-Schmidhauser, R., Gysel, M., Weingartner, E., Riccobono, F.,



1 Santos, S., Grüning, C., Faloon, K., Beddows, D., Harrison, R., Monahan, C., Jennings, S. G.,
2 O'Dowd, C. D., Marinoni, A., Horn, H.-G., Keck, L., Jiang, J., Scheckman, J., McMurry, P.
3 H., Deng, Z., Zhao, C. S., Moerman, M., Henzing, B., de Leeuw, G., Löschau, G. and
4 Bastian, S.: Mobility particle size spectrometers: harmonization of technical standards and
5 data structure to facilitate high quality long-term observations of atmospheric particle number
6 size distributions, *Atmospheric Measurement Techniques*, 5(3), 657–685, doi:10.5194/amt-5-
7 657-2012, 2012.

8 Yamartino, R. J.: A Comparison of Several “Single-Pass” Estimators of the Standard
9 Deviation of Wind Direction, *Journal of Climate and Applied Meteorology*, 23(9), 1362–
10 1366, doi:10.1175/1520-0450(1984)023<1362:ACOSPE>2.0.CO;2, 1984.

11 Yli-Juuti, T., Nieminen, T., Hirsikko, A., Aalto, P. P., Asmi, E., Hörrak, U., Manninen, H. E.,
12 Patokoski, J., Dal Maso, M., Petäjä, T., Rinne, J., Kulmala, M. and Riipinen, I.: Growth rates
13 of nucleation mode particles in Hyytiälä during 2003–2009: variation with particle size,
14 season, data analysis method and ambient conditions, *Atmos. Chem. Phys.*, 11(24), 12865–
15 12886, doi:10.5194/acp-11-12865-2011, 2011.

16

17

18

19

20

21

22

23

24

25

26

27

28

29

30

31

32



1 Table 1 Estimation of the median seasonal and annual CCN productions from NPF.

	CCN _{high} (cm ⁻³)	CCN _{med} (cm ⁻³)	CCN _{low} (cm ⁻³)
Dry season	3.96×10 ⁵	1.60×10 ⁵	9.40×10 ⁴
Wet season	8.48×10 ⁴	4.98×10 ⁴	3.90×10 ⁴
Whole year	4.81×10 ⁵	2.10×10 ⁵	1.33×10 ⁵

2

3

4 Table 2 Estimation of the median seasonal and annual CCN productions from NPF corrected
5 for the contribution of particles transported to the site.

	CCN _{high} (cm ⁻³)	CCN _{med} (cm ⁻³)	CCN _{low} (cm ⁻³)
Dry season	2.00×10 ⁵	7.71×10 ⁴	4.92×10 ⁴
Wet season	5.39×10 ⁴	2.13×10 ⁴	1.48×10 ⁴
Whole year	2.54×10 ⁵	9.84×10 ⁴	6.40×10 ⁴

6

7

8

9

10

11

12

13

14

15

16

17



1 Table 3 Description of the scenarios concerning the location of the station in the troposphere
 2 (boundary layer (BL), interface layer (IL) and free troposphere (FT)) during the first steps of
 3 the NPF process. The total number of occurrence is provided for each scenario in the second
 4 column. Since multiple events are frequently observed at Chacaltaya, a more detailed
 5 classification including the event position is specified in the last two columns.

Scenario	Description	Total number of occurrence	Single and first position events	Second and following events
S1	BL only	217	100	117
S2	IL only	9	6	3
S3	FT only	12	7	5
S4	FT first, IL following	13	13	0
S5	FT first, IL and then BL	11	11	0
S6	FT first, BL following	41	37	4
S7	IL first, BL following	20	18	2
S8	BL first, IL following	2	1	1
S9	BL first, FT following	1	1	0
S10	Random conditions	7	5	2

6

7

8

9

10



1

2

3

4 Table 4. CCN production as a function of the location of the station (BL or FT) at the onset of
 5 the NPF process.

Threshold CCN size	CCN increase for events started in the BL (cm ⁻³)			CCN increase for events started in the FT (cm ⁻³)		
	25 th perc.	Median	75 th perc.	25 th perc.	Median	75 th perc.
50 nm	2556	5072	10110	3070	5137	9378
80 nm	1155	2416	3919	1483	2138	5173
100 nm	820	1518	2338	960	1447	3568

6

7

8

9

10

11

12

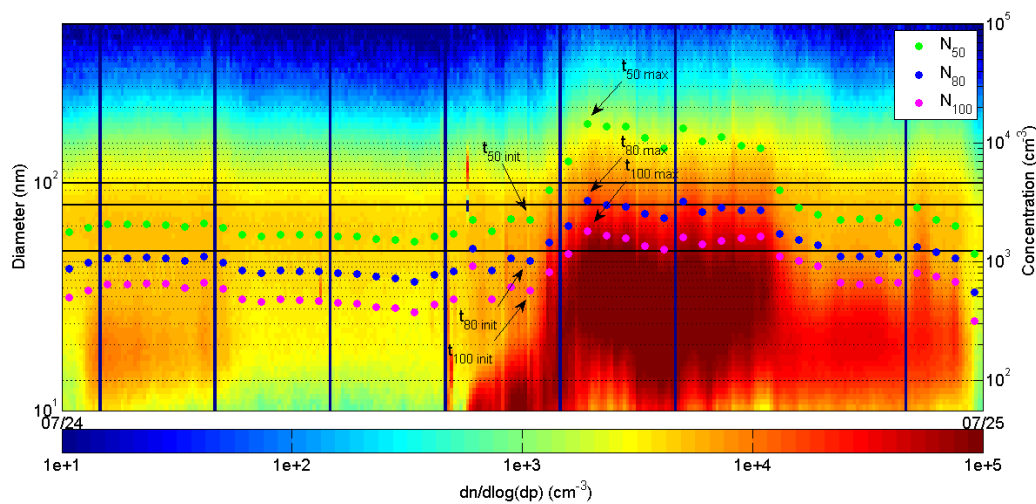
13

14

15

16

17



18

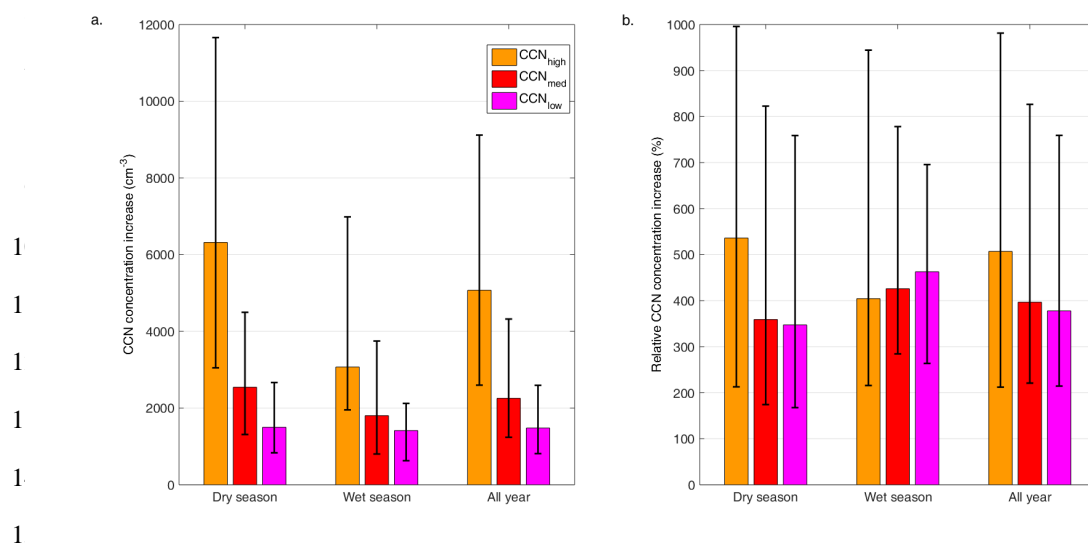
19

20

Fig. 1. Determination of the CCN concentration increase for the 3 threshold diameters (50, 80 and 100 nm). t_{init} and t_{max} denote, for each diameter, the times from which concentration increases are calculated. July 24th 2012, Chacaltaya.



1
2
3
4
5



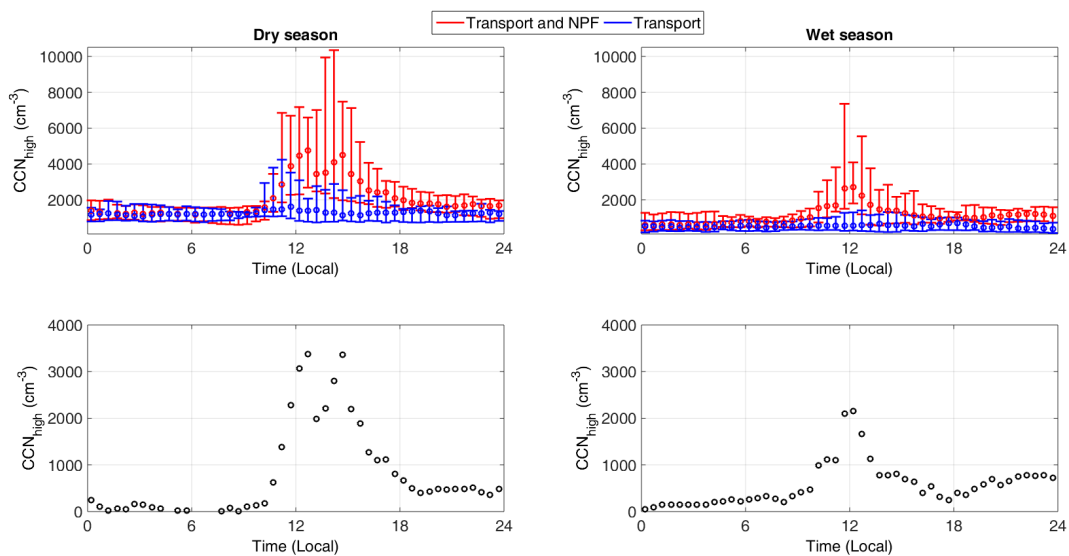
1

16 Fig. 2. Median a. absolute and b. relative CCN productions observed during type I events for
17 the different activation diameters and seasons. Lower and upper limits of the error bars stand
18 for the 1st and 3rd quartile, respectively. Chacaltaya, 2012.

19
20
21
22
23
24
25
26



1
2
3



14
15
16

17 Fig. 3. Median diurnal variation of CCN_{high} on event (upper panel, “Transport and NPF”) and
18 non-event days (upper panel, “Transport”). CCN_{high} attributed to NPF (lower panel) is
19 calculated as the difference of the concentrations recorded on event and non-event days.
20 Lower and upper limits of the error bars stand for the 1st and 3rd quartile, respectively.
21 Chacaltaya, 2012.

22
23
24
25
26
27



1
2
3
4
5
6
7
8
9
10
11
12
13
14
15
16
17
18
19
20
21
22
23
24
25
26

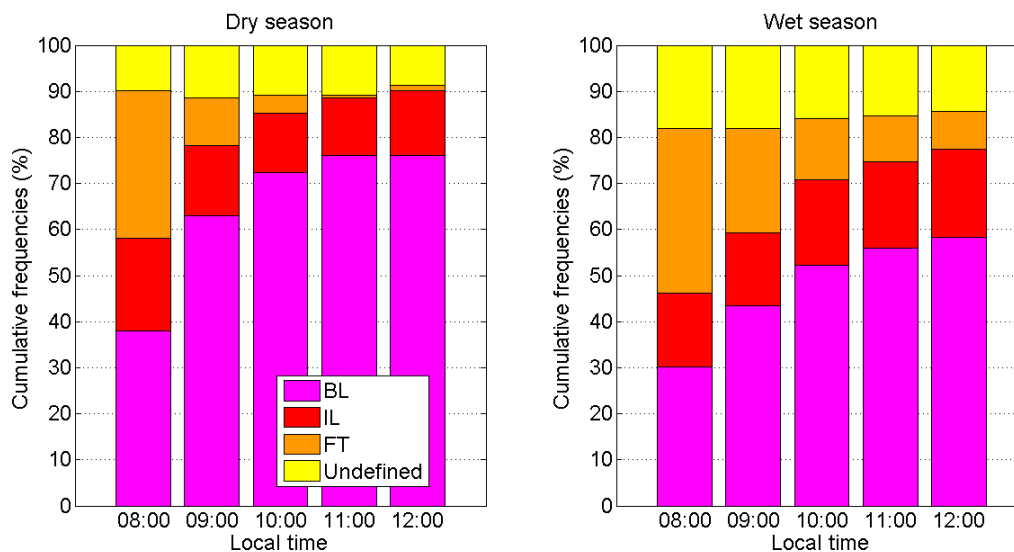
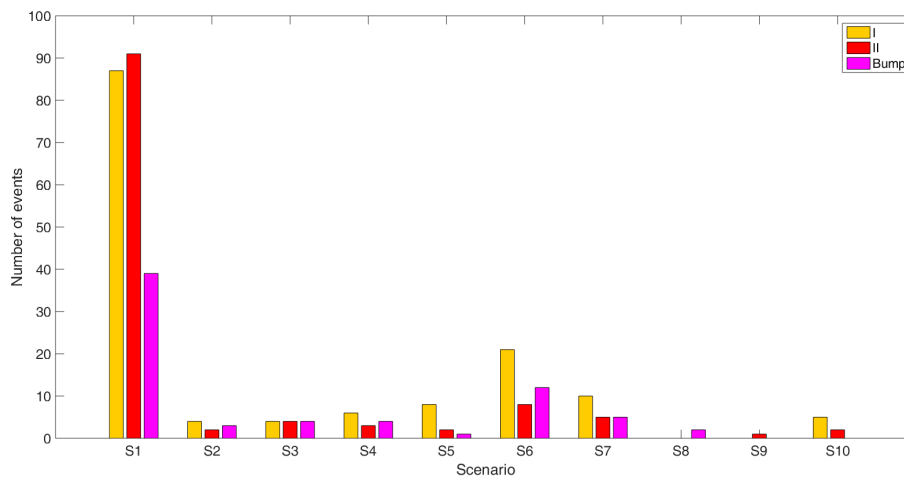


Fig. 4. Statistics on the location of the station in the tropospheric layers (boundary layer (BL), interface layer (IL) and free troposphere (FT)) between 8:00 and 12:00 (Local), separately for the dry and wet seasons. Chacaltaya, 2012.



1
2
3
4
5
6
7

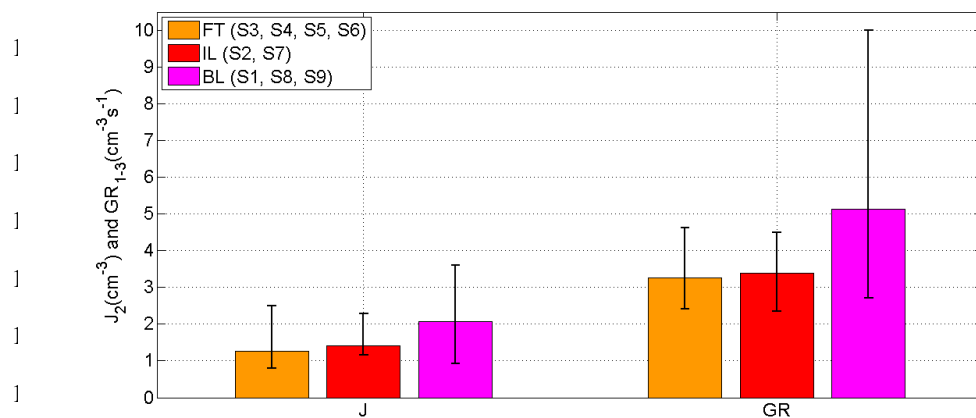


17 Fig. 5. Statistics on the event type (I, II or bump) as a function of the scenario describing the
18 location of the station in the tropospheric layers. Chacaltaya, 2012.

19
20
21
22
23
24
25
26



1
2
3
4
5
6
7
8



17

18 Fig. 6. Median particle formation and growth rates reported separately for type I events
19 initiated in the FT (scenarios S3, S4, S5 and S6), at the interface between the BL and the FT
20 (scenarios S2 and S7) and in the BL (scenarios S1, S8 and S9). Lower and upper limits of the
21 error bars stand for the 1st and 3rd quartile, respectively. Chacaltaya, 2012.

22